JOURNAL OF GEOPHYSICAL RESEARCH, VOL. 105, NO. C6, PAGES 14,261–14,272, JUNE 15, 2000

Residence time of inertial particles in a vortex

J. C. H. Fung

Department of Mathematics, Hong Kong University of Science and Technology, Hong Kong

Abstract. The residence time of a particle within a spatial domain is the total time it spends within this domain. We study the residence time of small dense particles in a spreading line vortex. Trajectories have been calculated for small dense particles released near a spreading line vortex. The results show that particles released far away from the vortex center will not be trapped by it, but particles released close to it will remain there for a considerable time. This residence time is shown to be a function of the particle inertia τ_p, its fall velocity V_T, and the vortex's Reynolds number Re_γ. The results of simulations also show that there is an optimum vortex Reynolds number such that the residence time of the particle is maximized within this simulated spreading line vortex. These findings are expected to be applicable to the coupling between the small-scale turbulent flow structures and the motion of the suspended particles.

1. Introduction

Suspended particles occur in many natural turbulent flows; in the atmosphere the residence times of various aerosols, such as man-made pollutants and water droplets falling under gravity, determine how long these aerosols remain suspended in air. A turbulent flow is not completely incoherent, i.e., consisting only of white noise; localized coherent motion (eddies or vortices) exists in the turbulent flow. The most important flow structures in connection with suspended particle are vortices [*Yule*, 1980; *Chung and Thoutt*, 1988; *Fung*, 1993, 1997, 1998; *Chan and Fung*, 1999; *Davila and Hunt*, 2000] because such vortices are able to trap particles temporarily and carry them along over considerable distances, eventually flinging them out as they start to decay.

Recent large-scale numerical simulations of turbulence, for example those of *Vincent and Meneguzzi* [1991], *Ruetsch and Maxey* [1991], and others, indicate strong organized structure in the form of long slender vortices ("worms") are present among the small scales of many turbulent flows. These vortices tend to be organized in tubes or ribbons of more or less elliptical cross section. Their radii appear to scale with the Kolmogorov microscale, and their lengths scale with the order of the integral scale of the flow. These vortex structures tend to persist over a long period of time, even when their length reaches the integral scale of the flow. These features have also been confirmed by direct numerical simulations of isotropic turbulence by *Jiménez et al.* [1993], who also showed that the typical core size δ of these vortical structures is $3\eta-5\eta$, where η is the Kolmogorov length scale and their circulation Γ increases with the vortex Reynolds number Re_γ. This discovery has generated considerable excitement in the turbulence community. One reason for this interest is that being strong and therefore presumably decoupled from the influence of other flow components, the behavior of the worms should be relatively easy to understand. Moreover, *Wang and Maxey* [1993] showed that the particle motion, in particular, the settling rate of particles, depends strongly on the small-scale vortical structures of the turbulent flow field, which occupy a small fraction of the fluid volume and provide a small fraction of the dissipation. Their results demonstrate that the maximum increase of particle settling rate occurs when the inertial parameters are comparable to the flow Kolmogorov scales. This Kolmogorov scaling indicates that the small-scale flow dynamics plays a significant role in certain aspects of particle transport in fully developed turbulence. The study indicates that the structural view of turbulent flows can contribute to the development of multiphase flow modeling, in addition to the more commonly used statistical view. These small-scale vortical structures can be modeled by a Burgers vortex [*Jiménez et al.*, 1993] or a spreading line vortex [*Vassilicos and Nikiforakis*, 1997], both of them incompressible solutions of the Navier-Stokes equation. Given the important role that the small scales play in the interaction between particles and turbulence and the prominence of vortex-like structures among these small scales, we investigate the motion of small inertial particles in a spreading line vortex here.

The paper is organized as follows. In section 2 the decay of a line vortex is considered, which leads to the diffusion of a localized vorticity distribution or to a spreading line vortex. In section 3 the equation of mo-

Paper Number 2000JC000260.
0148-0227/00/2000JC000260$09.00

tion for an inertial particle is described. In section 4 the simulation method and the results of the simulation of particle motion in a steady line vortex and in an unsteady spreading line vortex are presented.

2. Spreading Line Vortex

We consider a vortex filament in an incompressible fluid in which, initially, the vorticity is zero everywhere, except on the axis of the vortex filament with small core size ℓ_0 and with strength Γ at $t = 0$. Physically, this means that for small times, there is a narrow vortex core near the axis, and the rest of the flow field is irrotational. Vorticity is here diffused radially away from an initial concentration on a line, and we use cylindrical coordinates and take the z axis along the axis of the filament. Let u_r and u_θ be the radial and circumferential velocity components of the vortex, respectively; then $u_r = 0$, and the vorticity is governed by

$$\frac{\partial \zeta}{\partial t} = \nu\left(\frac{\partial^2 \zeta}{\partial r^2} + \frac{1}{r}\frac{\partial \zeta}{\partial r}\right), \tag{1a}$$

where

$$\zeta = \frac{\partial u_\theta}{\partial r} + \frac{u_\theta}{r}. \tag{1b}$$

The boundary condition is $u_\theta(r \to \infty, t > 0) \to 0$. The solution [see *Batchelor*, 1967] of (1) is

$$u_\theta(r,t) = \frac{\Gamma}{2\pi r}\left[1 - \exp\left(-\frac{r^2}{\ell^2(t)}\right)\right],$$

where $\ell^2(t) = \ell_0^2 + 4\nu t$; $\ell(t)$ is defined as the core size of the vortex at time t with an initial size of ℓ_0, and ν is the kinematic viscosity of the fluid. The dimensionless quantity Γ/ν is known as the vortex Reynolds number, based on the circulation of the vortices. This vortex Reynolds number Re_γ scales approximately as $Re_\gamma \sim 20\,Re_\lambda^{1/2}$ [*Jiménez et al.*, 1993; *Marcu et al.*, 1995], where Re_λ is the Reynolds number formed with the Taylor microscale. Note that near $r = 0$ the motion is a rigid body rotation. The streamlines are circles, and far away from the vortex, the velocity field decays as $1/r$. The intensity of the vortex decreases with time as the core spreads radially outward.

In the limit of large vortex Reynolds numbers, where $\Gamma/\nu \gg 1$, advection around the vortex is so fast that a fluid element may complete many turns around the vortex before $\ell(t)$ changes appreciably. In this paper we consider first the case where $\Gamma/\nu \gg 1$ and can therefore take a reference length L to be a time-independent characteristic length scale of the vortex flow [see *Ting and Klein*, 1991] and Γ/L to be the characteristic velocity. The nondimensional flow field has the form

$$u_r = 0, \tag{2a}$$

$$u_\theta = \frac{1}{2\pi r}\left[1 - \exp\left(-\frac{r^2}{\ell^2(t)/L^2}\right)\right]$$

$$= \frac{1}{2\pi r}\left[1 - \exp\left(-\frac{r^2}{r_0^2}\right)\right], \tag{2b}$$

where $r_0 = \ell(t)/L$ is a function of the initial core size and viscosity (or vortex Reynolds number). The corresponding velocity field in Cartesian coordinates becomes

$$u_x = -\frac{y}{2\pi r^2}\left[1 - \exp\left(-\frac{r^2}{r_0^2}\right)\right], \tag{3a}$$

$$u_y = \frac{x}{2\pi r^2}\left[1 - \exp\left(-\frac{r^2}{r_0^2}\right)\right]. \tag{3b}$$

Note that the center of vortex is chosen to be at the origin and L^2/Γ is the characteristic turnover time of the vortex over a characteristic length scale L.

In the case of moderate vortex Reynolds numbers the vorticity is diffused radially away from the initial concentration; hence the core size $\ell(t)$ of the vortex will increase with time. The velocity distribution of a spreading line vortex with different core sizes at different values of t are shown in Figure 1 as a function of r. The most obvious feature is that as r increases, u_θ increases to a certain maximum value and then decreases to zero as $r \to \infty$. Note that for large values of r ($\gg r_0$) the velocity distribution has the same form at all t. The value $r = r_m$ for which the maximum u_θ can be found is given by the solution of

$$1 + 2p = e^p,$$

where $p = (r_m/r_0)^2$. Note also that the maximum velocity u_θ is shifted away from the vortex center as the core size of the vortex (r_0) increases.

In this paper we consider the motion of a particle in a vortex flow in two cases: (1) a case with a very large Reynolds number where $\Gamma/\nu \gg 1$ and $\ell(t)$ can therefore be taken to be time-independent and (2) a case with different moderate vortex Reynolds numbers arrived at

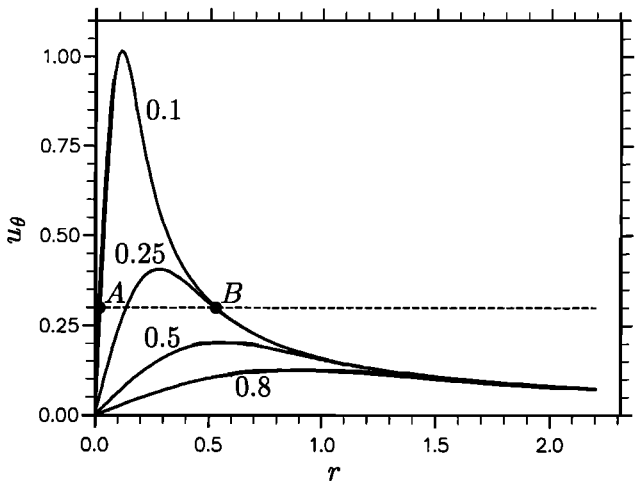

Figure 1. The velocity distribution associated with a spreading line vortex of different core sizes. The number indicates the core size of the vortex.

by changing the values of the viscosity ν, hence the core size of the vortex will be a function of time.

3. Equation of Motion for Inertial Particle

The motion of small spherical particles in a fluid is governed by particle inertia, gravity, and drag force (from the relative motion between the particle and the fluid). Assume that the particle concentrations are low, so that particle interactions can be neglected, and that the particles are sufficiently small relative to the smallest length scale in the turbulence (the Kolmogorov length scale $\eta = (\nu^3/\varepsilon)^{\frac{1}{4}} \simeq 1\text{mm}$ in the lower atmosphere), so that the relative motion approaching a particle is nearly a uniform flow. If, also, the particle time constant τ_p is short relative to the shortest timescales of the velocity field ($\tau = (\nu/\varepsilon)^{\frac{1}{2}} \simeq 0.08\text{s}$ in the atmosphere), then the fluid force on the particle is simply a Stokes drag force, and we can approximately determine the equation of motion [*Maxey*, 1987] as

$$m_p \frac{d\mathbf{v}}{dt} = 6\pi a\mu\,[\mathbf{u}(\mathbf{x}_p, t) - \mathbf{v}(t)] + m_p\mathbf{g}\,, \qquad (4)$$

where $\mathbf{u}$ is the fluid flow field and m_p, a, μ and g are the particle mass, particle radius, fluid viscosity, and gravitational acceleration constant, respectively. As the particle moves along its trajectory $\mathbf{x}_p(t)$ in the flow field $\mathbf{u}(\mathbf{x}, t)$, its velocity will change continuously in response to the changes in the local fluid velocity $\mathbf{u}(\mathbf{x}_p, t)$. Equation (4) is a simplified version of the more general equation of motion [*Maxey and Riley*, 1983; *Hunt et al.*, 1988]. Previous experience indicates that Stokes drag gives qualitatively similar results as some nonlinear empirical drag law [*Wang and Maxey*, 1993; *Fung*, 1998] if the particle Reynolds number is small. A Stokes drag is assumed here. Despite the restrictions that have been imposed, (4) is applicable to many different problems, such as aerosols in gases and small particles in water. (For typical solid particles in air, for example, $V_T \lesssim 0.2\,\text{m}\,\text{s}^{-1}$, corresponding to particle radii less than 50 μm.)

The equation is scaled by the characteristic velocity and the characteristic length scale of the flow, namely, Γ/L and L. Nondimensional variables are introduced as follows:

$$x^* = \frac{x}{L}, \quad \mathbf{x}_p^* = \frac{\mathbf{x}_p}{L}, \quad t^* = \frac{tL^2}{\Gamma},$$

$$\mathbf{v}^* = \frac{\mathbf{v}L}{\Gamma}, \qquad \mathbf{u}^* = \frac{\mathbf{u}L}{\Gamma}.$$

The scaled form of (4), with the asterisks suppressed, is

$$\tau_p \frac{d\mathbf{v}}{dt} = \mathbf{u}(\mathbf{x}_p, t) - \mathbf{v}(t) + \mathbf{V}_T\,, \qquad (5)$$

where the two governing dimensionless parameters are the scaled dimensionless Stokes settling velocity for still fluid

$$V_T = \frac{m_p g L}{6\pi a\mu\Gamma} \sim \frac{w_0}{\Gamma/L}\,, \qquad (6a)$$

where $w_0 = m_p g/6\pi a\mu$ (the settling velocity in still fluid) and the dimensionless inertia parameter

$$\tau_p = \frac{m_p\Gamma}{6\pi a\mu L^2} \sim \frac{w_0}{\Gamma/L}\,\frac{\Gamma^2}{gL^3} = \frac{w_0\Gamma}{L^2}\,, \qquad (6b)$$

which measures the dimensionless response time of the particle motion to changes in the velocity of the surrounding fluid. The importance of particle inertia in a given situation is determined by the value of τ_p: when τ_p is small, the inertial term is small, and the particle responds rapidly to changes in the surrounding flow field, while if the value of τ_p is large, the particle inertia has a strong influence on the particle motion. Even if we assume a force linear in velocity, solving the equation of motion is still a complex problem because of the nonlinear dependence of $\mathbf{u}(\mathbf{x}_p, t)$ on the particle position.

In this study, we find that particle inertia and the vortex Reynolds number have some important effect on the residence time of the particle. Physically, the effect of particle inertia is to limit the response of the particle to the rapid changes in the local fluid velocity and hence to produce a phase lag between the two.

4. Simulation Method and Results

The motion of a particle is found by numerically solving the equation of motion (5) using the fourth-order Runge-Kutta method with an adaptive step size control. This method will automatically adjust the step size to control the truncation error with a prescribed tolerance. For each simulation a flow field is generated as described in section 2. The particles are released with initial velocity $\mathbf{v}(0) = (0, V_T)$.

Before discussing the general results corresponding to the parametric study of the residence time of the particle inside the trapping region, which is a function of the three governing parameters τ_p, V_T, and ν, we will discuss how to define the trapping region of a spreading line vortex and show that it is a function of V_T and r_0.

4.1. Particle Motion

4.1.1. Particles without inertia. In the limit of a very large vortex Reynolds number the core size of the vortex can be regarded as a constant in time, i.e., $\ell(t) = \ell_0$, and some useful results can be obtained by considering the simplified case in which the particle inertia tends to zero, i.e., $\tau_p \to 0$. In this case the fluid drag force on the particle balances at every instant the force due to gravity; that is, the net force on the particle is zero. This implies that the right-hand side of (5) vanishes, that the particle is everywhere moving vertically at its settling velocity relative to the ambient fluid velocity, and that its trajectory $\mathbf{x}_p(t) = (x, y)$ is determined by the solution of

$$\mathbf{v}(t) = \mathbf{u}(\mathbf{x}_p, t) + \mathbf{V}_T \tag{7}$$

and the specification of its initial position. Therefore the velocity components of the particle are

$$\frac{dx}{dt} = u_x \tag{8a}$$

$$\frac{dy}{dt} = u_y - V_T\,. \tag{8b}$$

Following the work of *Maxey* [1987], a "particle velocity field" can be defined that is incompressible and can be expressed in terms of a "particle stream function,"

$$\psi_p = \psi + V_T x\,,$$

where ψ is the stream function of fluid velocity. The trajectory of a particle is a curve along which ψ_p is a constant. However, in this case, ψ cannot be expressed analytically.

Another useful way to view the motion of the particles is to follow the paths of a line of particles initially distributed uniformly far above the vortex with some particles released closed to the center of the vortex. Figure 2 shows such particle trajectories. The obvious feature is that for $V_T < \max(u_\theta)$, there is a possibility of permanent particle suspension, with particles executing closed orbits about a point on the x axis. Regions where particles exhibit endless closed orbits are called trapping regions. Any particle already in this region of closed orbits will stay there indefinitely, and any particle outside that region will never enter it. The trajectories more remote from the center of the vortex are not closed. Particles placed on one of these trajectories are rapidly swept through the vortex with no possibility of suspension. The largest closed orbit, or the streamline which separates the region of particle trapping from the rest of the flow, is called the bounding trajectory (the dashed line in Figure 2), and it starts at the saddle point B on the particle trajectory [see *Maxey and Corrsin*, 1986]. A similar particle path in a Rankine vortex was also obtained by *Nielsen* [1984, Figure 3]. In two dimensions the existence of such a trapping region containing closed trajectories implies the presence of equilibrium points at which the local flow velocity is equal and opposite to the falling velocity, i.e., $\mathbf{u}(\mathbf{x}_p, t) + \mathbf{V}_T = \mathbf{0}$, so that a particle there would remain at rest. Therefore, by setting the particle velocity $\mathbf{v}(t) = (0, 0)$ one can then solve (8) given (3) for all the locations where equilibrium is achieved for the particle, stably or not. From (8a) the y location of the equilibrium points are always located at $y = 0$, and from (8b) the corresponding x coordinates can be obtained by numerically solving

$$\frac{1}{x}\left[1 - \exp\left(-\frac{x^2}{r_0^2}\right)\right] - V_T = 0 \tag{9}$$

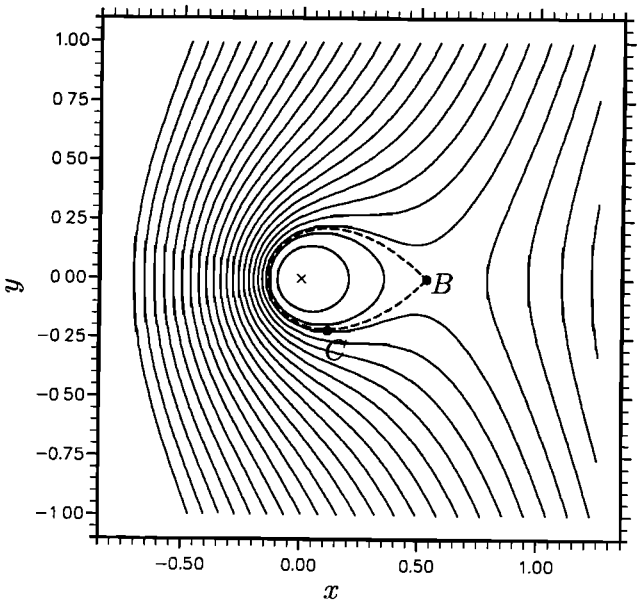

Figure 2. The trajectory field for $V_T < \max(u_\theta)$. The dashed line represents the bounding trajectory; the cross represents the center of the vortex; B is the saddle point; and C is the lowest point of the bounding trajectory.

for x. Equation (9) has two parameters, the settling velocity V_T and the core radius r_0. Alternatively, the solutions to (9) can be plotted versus u_θ values (see Figure 1). The different velocity distribution curves correspond to different values of core radius r_0 of the vortex, as indicated. Such a velocity distribution curve intersected with a constant u_θ line yields the x (or radial) position of the equilibrium locations (since when $y = 0$, $u_x = u_\theta$), of which there are none if $V_T > \max(u_\theta)$, one if $V_T = \max(u_\theta)$, or two if $V_T < \max(u_\theta)$. Note that we are only interested in the larger value of the intersection point (the point B in the case $V_T < \max(u_\theta)$) since we want to find the largest closed orbit, i.e., the bounding trajectory.

For illustration purposes, let us study the solutions for $V_T = 0.3$ and $r_0 = 0.1$, in which case $V_T < \max(u_\theta) \approx 1.0$. From Figure 1 one can see that the curve of the velocity distribution with $r_0 = 0.1$ intersects line $u_\theta = 0.3$ at two points (A and B). Hence there are two solutions for x, from which one can numerically compute the coordinates of these two equilibrium points A and B using (9). Both the equilibrium points A (located at small radius in the proximity of the center of vortex) and B (located far away from center of vortex) are saddle points that are unstable. Note that both these points are located at the upflow region of the vortex. The bounding trajectory, which separates the region of particle trapping from the rest of the vortex (dashed line in Figure 2) starts at a saddle point B. For smaller values of V_T the trapping region is larger (since the point B is farther away from the vortex center). In

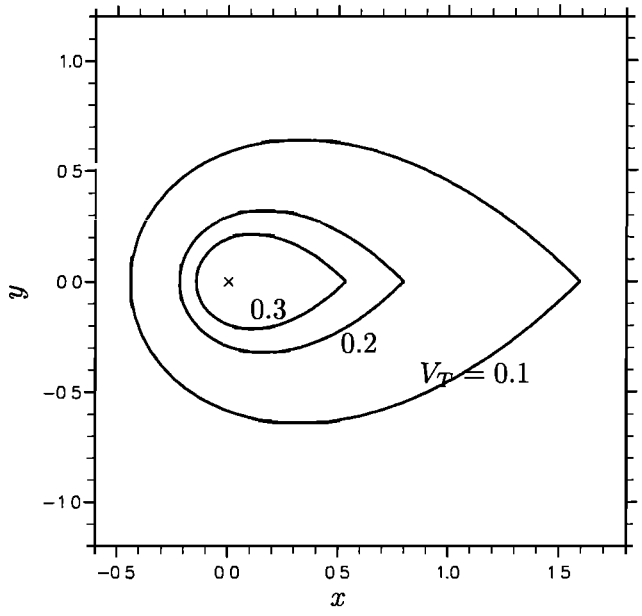

Figure 3a. The size of the trapping region decreases as the settling velocity of the particle (V_T) increases from 0.1 to 0.3 with $\ell_0 = 0.1$. The cross represents the center of the vortex.

the limit V_T tends to zero all particles would be trapped and suspended inside the vortex. Note that no trapping region exists when $V_T = \max(u_\theta)$.

From (9) we can conclude that the shape and size of the trapping region of the vortex, L_v (defined as the horizontal length of the trapping region (the dashed line in Figure 2) when $y = 0$) is a function of the settling velocity V_T and the core size of the vortex r_0. We will show that the residence time of the particle is a function of V_T and r_0 too. Similarly, the height of the bounding trajectory, L_h, can also be defined as the vertical distance between the center of the vortex and the lowest point of the bounding trajectory, i.e., the point C in Figure 2 (see also Figure 8c).

Figure 3a shows the shapes and sizes of the bounding trajectories with three different values 0.1, 0.2, and 0.3 for the settling velocity V_T of the particle and with a fixed value of the core size $\ell(t) = \ell_0 = 0.1$. Figure 3b shows the corresponding sizes of the trapping region, L_v, versus V_T, showing that the size of the trapping region becomes smaller as V_T increases (the point B moves closer to the center of the vortex). The trapping region disappears at $V_T = \max(u_\theta)$.

For a finite vortex Reynolds number Γ/ν the core size of the vortex increases with time since the vorticity is diffused radially outward. Therefore the size of the trapping region changes with time too for a fixed value of the settling velocity of the particle. Figure 4a shows the shapes and sizes of the trapping regions with three different values for the vortex core sizes $\ell(t) = 0.1$, 0.2, and 0.3 and with a fixed value of $V_T = 0.3$. Figure 4b shows the corresponding sizes of the trapping region, L_v, versus the core size $\ell(t)$. From Figure 4a one can see that despite the core size of the vortex increasing with time (see Figure 1) the size of trapping region decreases and shifts to the right with time.

These closed trajectories are similar in many ways to those found by *Nielsen* [1984] in his study of oscillating flow over sand ripples. At certain times in the wave cycle a recirculating vortex forms behind the ripple, and sand particle streamlines in the vortex are closed. The simplified drag-buoyancy equation (8) does not account for the drift of particles caused by inertia effects and cannot predict the continuous trapping of fresh particles by a vortex, which is observed in experiments [*Yule*, 1980]. To determine the existence of this trapping of particles even with inertia, (5) with inertia effects must be used.

In order to obtain a feeling for typical particle sizes that might be trapped by the stretched Burgers-like or spreading line vortices observed at the small scales of turbulent flows, *Marcu et al.* [1995] obtained a criterion for the maximum radius of the particle,

$$d_{\text{trap}} = 10\eta\sqrt{\frac{1}{\gamma Re_\lambda}}, \tag{10}$$

that might be trapped. Here $\gamma = \rho_p/\rho_f$ is the density ratio between the particle and its surrounding fluid. For a typical laboratory experiment [*Browne et al.*, 1983], with $Re_\lambda = 190$ and $\eta = 0.16$ mm, (10) gives $d_{\text{trap}} \approx 4$ μm for water droplets in air with $\gamma = 1000$ or $d_{\text{trap}} \approx 71$ μm for sand particles in water with $\gamma = 2.65$. A typical atmospheric flow [*Wyngaard*, 1992], on the other hand, is characterized by $Re_\lambda \approx 10^4$ and $\eta = 1$ mm, giving $d_{\text{trap}} \approx 3.5$ μm for coal particles in air with $\gamma = 833$ and $d_{\text{trap}} \approx 3.1$ μm for water droplets in air with $\gamma = 1000$.

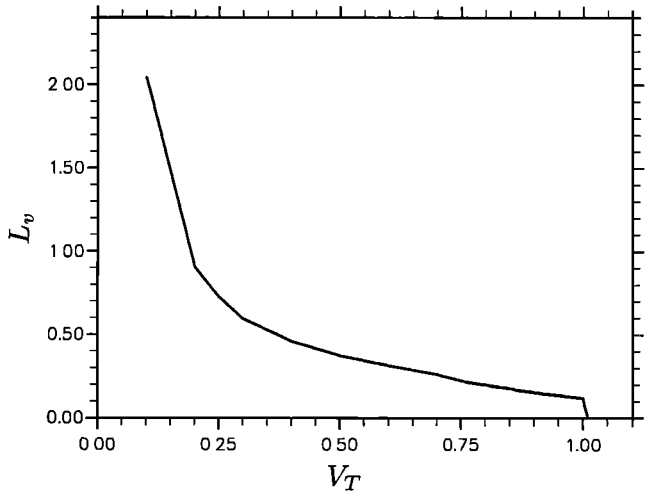

Figure 3b. Plot of the size L_v of the trapping region as a function of V_T corresponding to Figure 3a. Note that when $V_T = \max(u_\theta)$, the trapping region disappears.

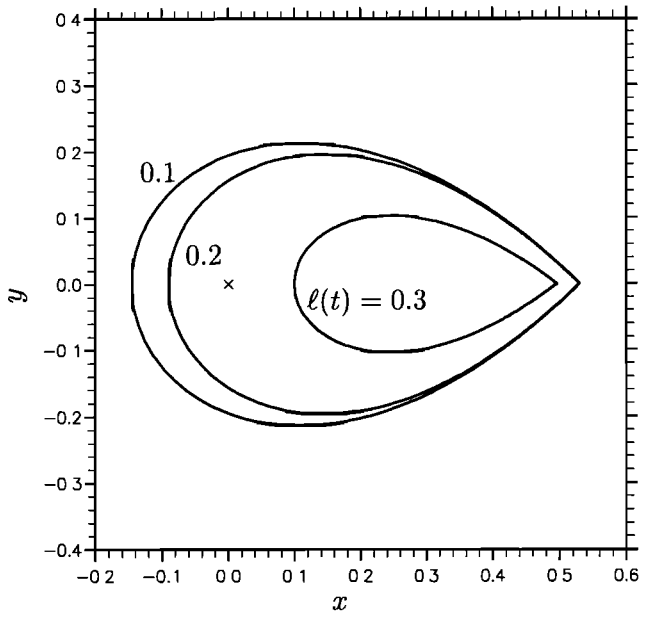

Figure 4a. The size of the trapping region decreases as the core size of the vortex ($\ell(t)$) increases from 0.1 to 0.3 with a fixed value of $V_T = 0.3$. The cross represents the center of the vortex.

As far as the vortices observed at the small-scale turbulent air flow are concerned, only small particles with sizes of 4-71 μm can be trapped in a typical laboratory experiment ($Re_\lambda = 190$), and those with sizes ~ 4 μm can be trapped in atmospheric flow ($Re_\lambda = 10^4$). Therefore one would expect that only small particles with sizes ~ 4 μm might be trapped by this spreading line vortex, which is observed at the small scale of turbulent flows.

4.1.2. Particles with inertia. Without particle inertia and with $V_T < \max(u_\theta)$, particles can be trapped in the trapping region permanently, that is the residence time is infinitely long. In the presence of particle inertia the motion of a particle is determined by (5). Some typical trajectories with different inertia parameters τ_p for a very large vortex Reynolds number $Re_\gamma \to \infty$ (in this case the core size of the vortex can be regarded as constant in time; hence the trapping region is constant in time too) are shown in Figure 5. In none of these trajectories do we see a permanently closed orbit corresponding to a trapping particle even when the particles are initially located in the trapping region. However, when the particles are released inside the trapping region, they remain there for a considerable time and then slowly spiral outward and eventually leave the trapping region (Figures 5b, 5d, and 5f). An approximate analytical account of this process without particle inertia in a Rankine vortex was also given by *Nielsen* [1984]. In all of these cases, no new particles can enter the trapping region. It seems perhaps counterintuitive that the higher the inertia of the particle, the quicker the particle leaves the trapping region. This can be easily explained when we consider the effect of particle inertia on moving objects: particles with inertia do not turn easily. The outward inertial centrifugal force acting normal to the trajectory is always larger than the inward radial drag force. Hence the particle is driven by the flow away from the vortex center. Therefore one of the effects of particle inertia is to destroy closed orbit, and this will likely have an important effect on the residence time of the particle.

Figures 5a, 5c, and 5e show that outside the trapping region, there is a critical dividing trajectory; particles released on one side of it pass on the downflow side of the vortex where the particle is being accelerated; particles released on the otherside pass on the upflow side where the particle is being decelerated. The separation of particle trajectories on the downflow side of the vor-

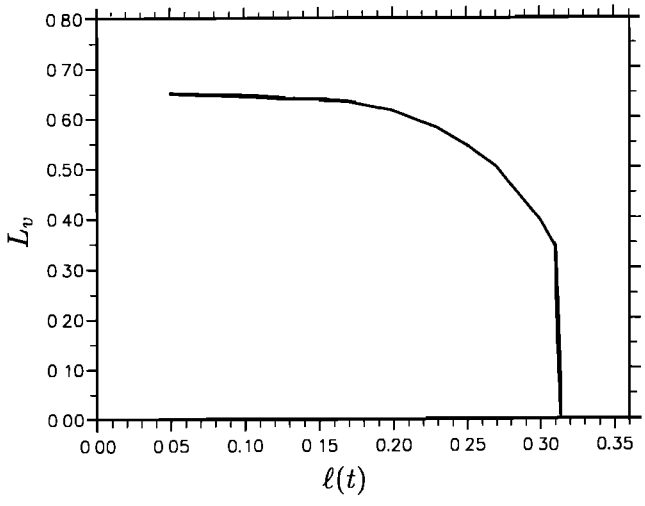

Figure 4b. Plot of the size L_v of the trapping region against $\ell(t)$ corresponding to Figure 4a. Note that the trapping region suddenly vanishes when the core size of the vortex increases to ~ 0.314.

Figure 5. The particle trajectories obtained by solving (5) with fixed values of $V_T = 0.3$ and $\ell(t) = \ell_0 = 0.1$ and with three different values of the inertia parameters: (a) and (b) $\tau_p = 0.004$, (c) and (d) $\tau_p = 0.04$, and (e) and (f) $\tau_p = 0.4$. The dashed line represents the bounding trajectory and the cross represents the center of the vortex. Figures 5a, 5c, and 5e show the trajectories of particles initially released outside the trapping region, and figures 5b, 5d, and 5f show those of particles initially released at the center of the vortex. Note that the trapping region is independent of the inertia of the particle.

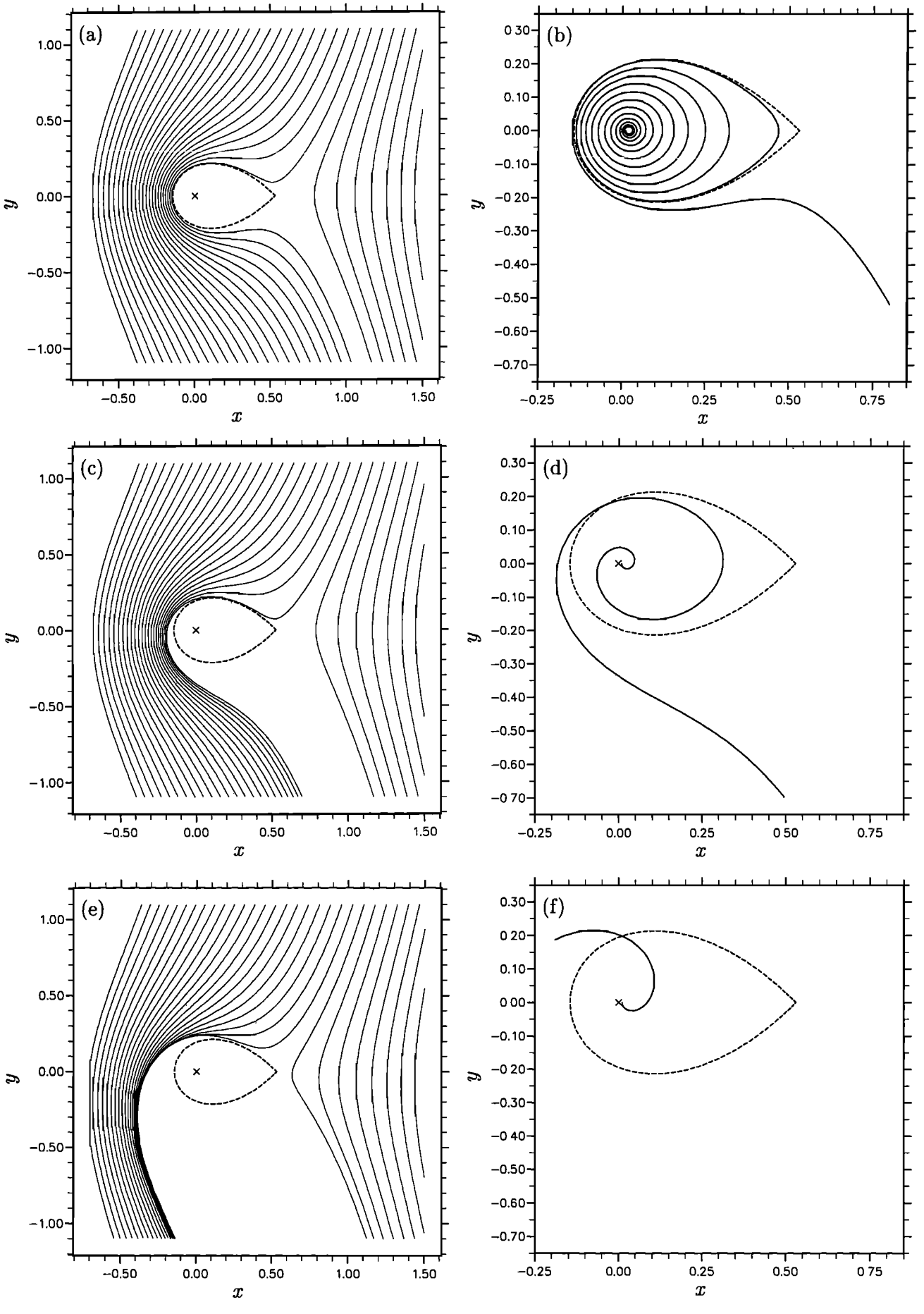
(a)
(b)
(c)
(d)
(e)
(f)
x
y

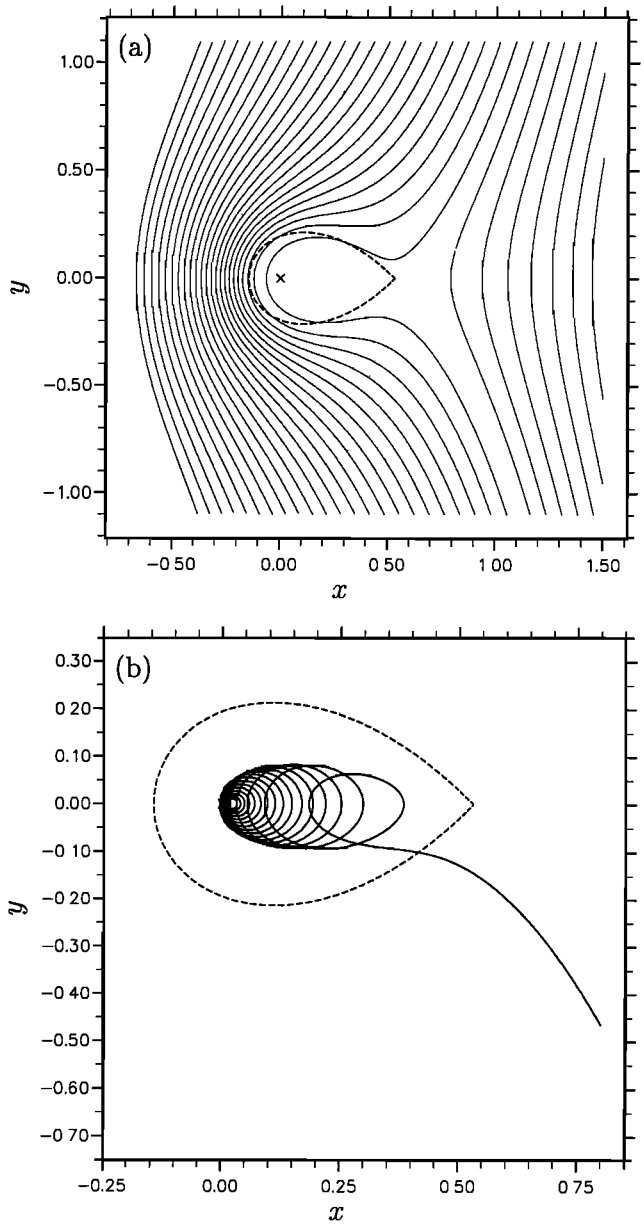

Figure 6. The particle trajectories with fixed values of $V_T = 0.3$, $\tau_p = 0.004$, $\ell_0 = 0.1$, and $\nu = 0.0007$ in a spreading vortex with core size changing with time. The dashed line represents the bounding trajectory at time $t = 0$ with an initial core size $\ell_0 = 0.1$, and the cross represents the center of the vortex. (a) The particles are initially released outside the trapping region, and (b) the particle is initially released at the center of the vortex.

tex is very much reduced as they pass round the vortex; simulation results show that particle accelerations are large, and there is considerable interparticle shear. Notice that there is a region of space below the vortex that the particles cannot enter, and this region of space becomes larger as the inertia of the particle increases from 0.004 to 0.4.

For a moderate vortex Reynolds number the core size of the vortex increases with time. However, the size of the trapping region decreases with time. Figure 6a shows the trajectories of particles released far away above a growing vortex center with $\nu = 0.0007$. The general feature is similar to that of Figure 5a. Figure 6b shows the trajectory of a particle released at the center of the same growing vortex. The particle not only shows an outward spiral motion but also shifts to the right since the trapping region also drifts to the right and becomes smaller as time increases (see also Figure 4). There is also a slow drift to the left that *Nielsen* [1984] predicted.

These trapping features are not limited to this spreading line vortex. For example, *Nielsen* [1984] and *Perkins and Hunt* [1995] considered the velocity field of a Rankine vortex and showed that there are regions where particles follow a closed trajectory.

4.2. Residence Time of the Particle

The residence time T_p of a particle can be defined as the total time for which the particle remains trapped inside the trapping region if released at the center of a vortex. The size of the trapping region is a function of the particle properties and the size of the vortex. Our results show that it depends on the three dimensionless parameters, particle inertia τ_p, settling velocity of particle V_T, and vortex Reynolds number Re_γ $(= \Gamma/\nu)$. In this section we will consider the effect of (1) varying the settling velocity of the particle while keeping τ_p and Re_γ constant, (2) varying τ_p while keeping V_T and Re_γ constant, and (3) varying the vortex Reynolds number while keeping τ_p and V_T constant.

4.2.1. Fixed values of τ_p and Re_γ. The residence times of the particle T_p inside the trapping region of the vortex have been computed for different values of V_T for $Re_\gamma \to \infty$ $(\nu \to 0)$ and for three different fixed values of τ_p (see Figure 7). The most obvious feature is that the residence time decreases monotonically

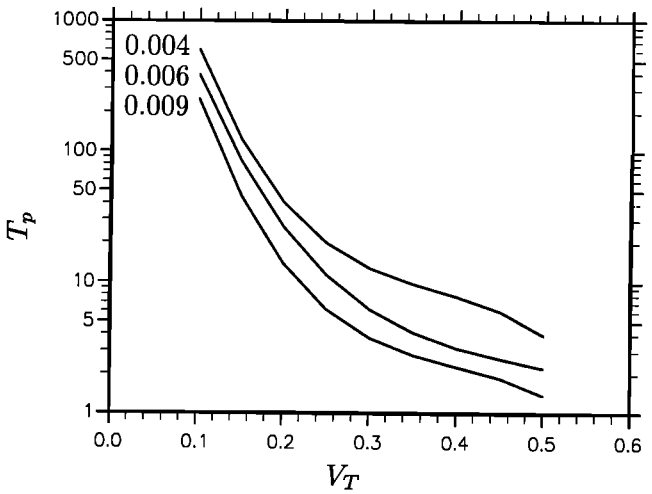

Figure 7. Linear log plot of the residence time T_p of the particle versus V_T with three different values of inertial parameters $\tau_p = 0.004$, 0.006, and 0.009.

with V_T. This is because the particle cuts through the vortex faster for larger values of V_T. This monotonic decrease is easily anticipated from the result $t_s = g/w_0\Omega^2$ *Nielsen* [1984, equation (57)] for the spiralling timescale of a particle in a solid core vortex with angular frequency Ω. Also, note that the larger the value of τ_p (higher inertia), the smaller the value of T_p for all fixed values of V_T since the centrifugal force increases (or the particle spirals out faster) as τ_p increases. The same simulations as above were also carried out with moderate vortex Reynolds numbers (i.e., $\nu \neq 0$), and similar results for T_p were also observed.

4.2.2. Fixed value of V_T and Re_γ. The influence of τ_p on the residence time of the particle inside the trapping region for a fixed value of $V_T = 0.3$ and for $Re_\gamma \to \infty$ ($\nu \to 0$) is also investigated (Figure 8a). The residence time T_p (solid line) no longer decreases monotonically as τ_p increases. T_p now oscillates with τ_p. This can be explained by counting the number of turns, N_c, the particle makes or, equivalently, by counting how many times the trajectory of the particle cuts across the positive x axis before leaving the trapping region.

From Figure 8a we can see that whenever the residence time T_p decreases, N_c decreases too, but whenever the residence time T_p increases, N_c remains constant. This can be explained by looking at two typical ranges of τ_p in Figure 8a. For example, as τ_p increases from 0.0075 to 0.0085, N_c (the dashed line) remains unchange at 5 while the residence time increases. This is because the particle spirals out of the trapping region faster as τ_p increases and at the same time, the distance between the particle trajectory with $\tau_p = 0.0085$ and the vortex center becomes larger compared with that for $\tau_p = 0.008$, while both of them make the same number of turns ($N_c = 5$) inside the trapping region before they escape. Note also that the larger the radius of the circulation of the particle around the vortex center, the longer it will take for the particle to complete a turn (smaller spiraling rate) since the motion of the particle will be slower as u_θ decreases with increasing r (for $r > r_m$). Therefore the particle will spend more time inside the trapping region as τ_p increases in this range. This situation can be clearly seen in Figure 8b with two particle inertia parameters of $\tau_p = 0.008$ and $\tau_p = 0.0085$. A particle with $\tau_p = 0.0085$ clearly has a larger radius of circulation than one with $\tau_p = 0.008$.

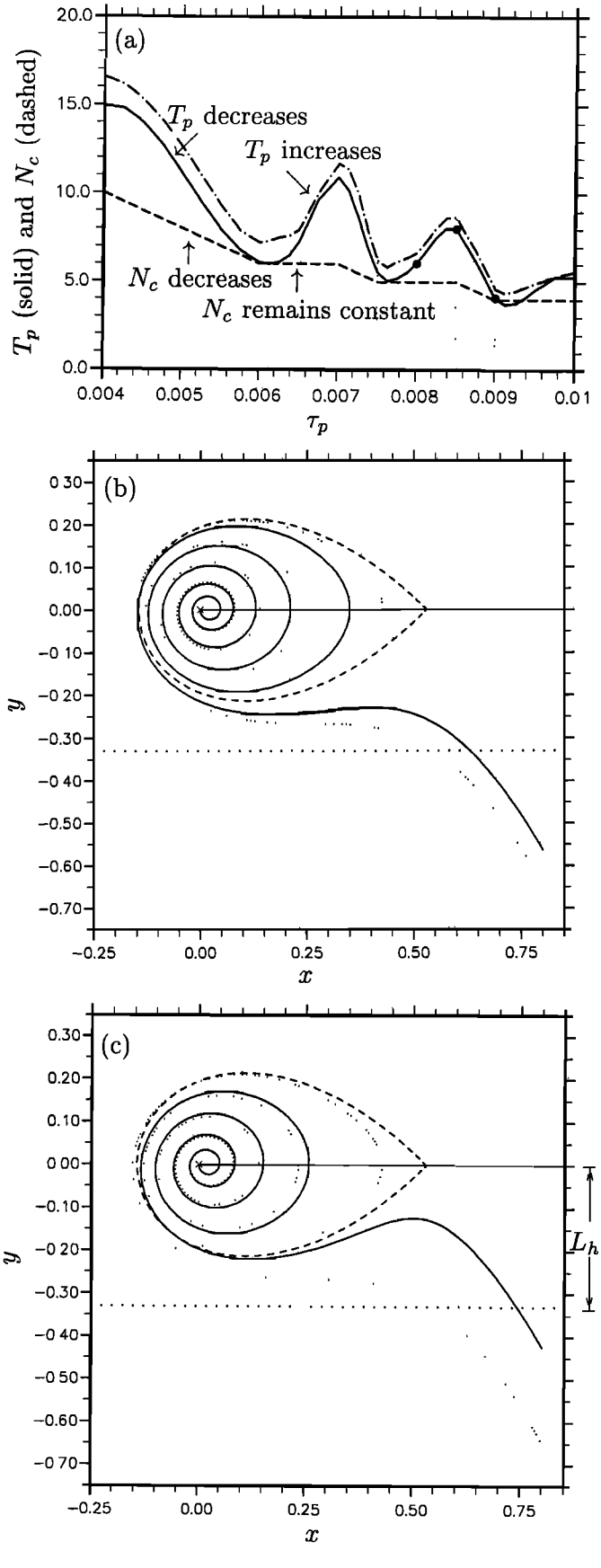

Figure 8. (a) The residence time of the particle (solid line) and the number of turns N_c the particle makes inside the trapping region (dashed line) as functions of τ_p in a steady vortex. The dash-dotted line represents the alternative residence time T_p' of the particle. (b) and (c) Two particle trajectories with two different inertial parameter τ_p obtained by solving (5) with fixed values of $V_T = 0.3$ and $\ell(t) = \ell_0 = 0.1$ in a vortex. The particles are released at the center of the vortex, which is inside the trapping region. The dashed line represents the bounding trajectory and the cross represents the center of the vortex. In Figure 8b the solid line is for $\tau_p = 0.008$, and the dotted line is for $\tau_p = 0.0085$. In Figure 8c the solid line is for $\tau_p = 0.009$, and the dotted line is for $\tau_p = 0.0085$.

However, as τ_p increases from 0.0085 to 0.009, N_c decreases from 5 to 4, and the residence time decreases too. This is because the particle with $\tau_p = 0.009$ makes one less turn, compared to the one with $\tau_p = 0.0085$ inside the trapping region, before it escapes (see Figure 8c).

One may ask whether this oscillation of residence time may be merely a result of our specific definition of the residence time since we use the trapping region of inertialess particle for the residence time calculation of finite inertia particles. Therefore an alternative definition of the residence time T_p' is the time it takes for a particle to settle a distance $1.5L_h$ below the vortex center (see Figure 8c), where L_h is the height of the bounding trajectory that was defined in section 4.1. This definition is taken from Figure 8c, which shows that the larger inertia particle, after escaping from the trapping region, will move up more before it settles permanently. In Figure 8a the computed alternative residence time T_p' (dash-dotted line) of the particle is also plotted. It is clear that a similar oscillatory result with τ_p is obtained and that the locations of the crest and trough occur at more or less those of T_p, but T_p' tends to have larger values purely because the particle will take a longer time to fall below $1.5L_h$, compared with just getting out of the bounding trajectory. Therefore we can conclude that the oscillatory behavior of the residence time T_p with τ_p is genuine and not an artifact of our definition of the residence time.

In the case of a moderate vortex Reynolds number with $\nu = 0.001$ the relationships between τ_p, the residence time T_p, and the alternative residence time T_p' are shown in the Figure 9a. Figure 9a shows similar features to those of the steady vortex. The reason for the oscillating residence time is similar to that of the steady vortex: the particle with the larger τ_p makes a slightly bigger spiral from the center of the vortex or makes one less turn before it escapes from the trapping region (see Figures 9b and 9c).

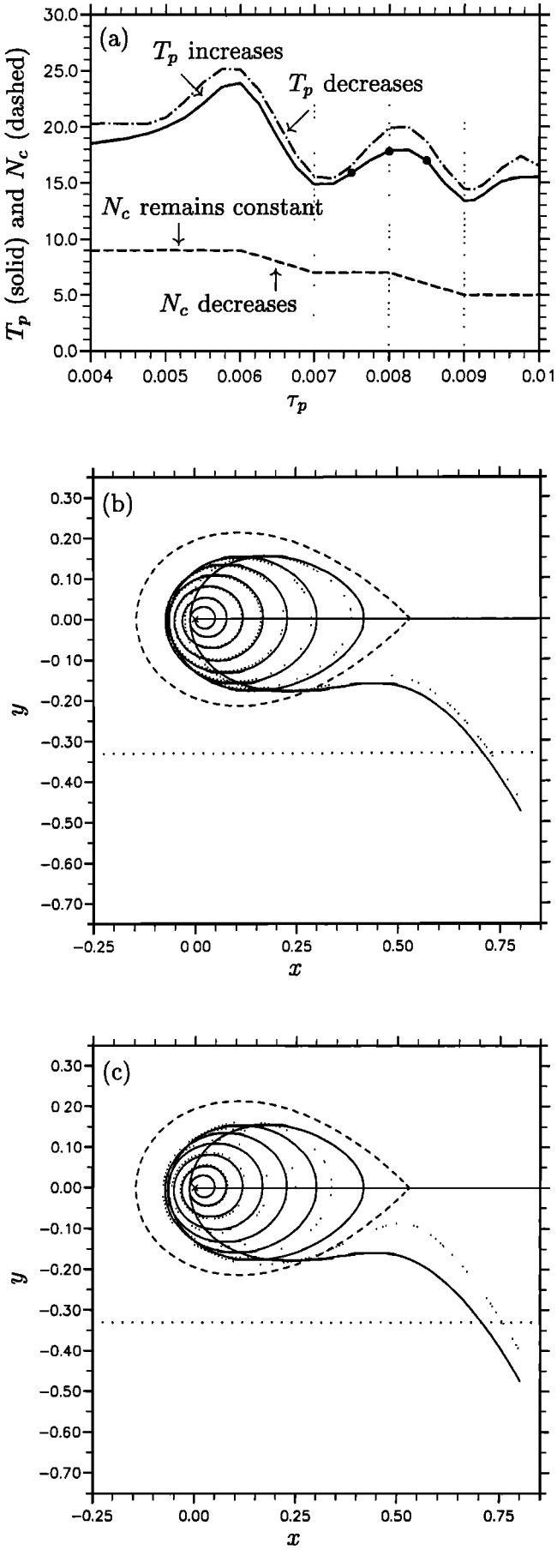

Figure 9. The residence time of the particle (solid line) and the number of turns N_c the particle makes inside the trapping region (dashed line) versus τ_p in a spreading vortex with $V_T = 0.3$, $\ell_0 = 0.1$, and $\nu = 0.001$. The dash-dotted line represents the alternative residence time T_p' of the particle. (b) and (c) The corresponding two particle trajectories with two different inertial parameter τ_p obtained by solving (5) with fixed values of $V_T = 0.3$, $\ell_0 = 0.1$, and $\nu = 0.001$ in a spreading vortex. The particles are released at the center of the vortex, which is inside the trapping region. The dashed line represents the bounding trajectory, and the cross represents the center of the vortex. In Figure 9b the solid line is for $\tau_p = 0.008$ and the dotted line is for $\tau_p = 0.0075$. In Figure 9c the solid line is for $\tau_p = 0.008$, and the dotted line is for $\tau_p = 0.0085$.

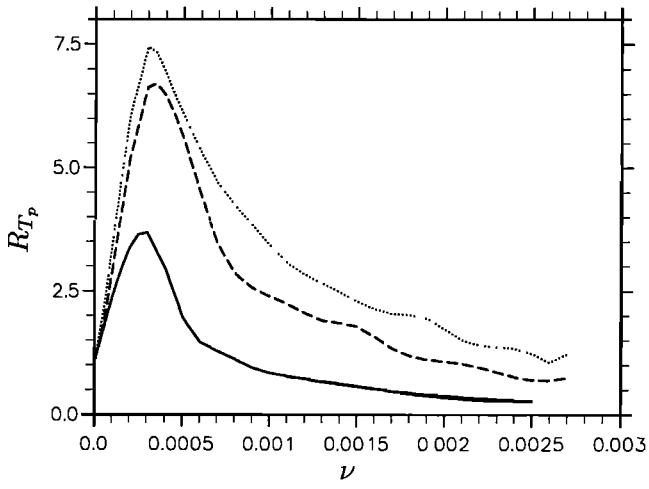

Figure 10. The ratio of the residence time of the particle versus ν in a spreading line vortex with $V_T = 0.3$, $\ell_0 = 0.1$, and three different values of particle inertia $\tau_p = 0.003$ (solid), 0.006 (dashed), and 0.009 (dotted).

4.2.3. Changing the vortex Reynolds number. Of interest is the dependence of the residence time T_p on the vortex Reynolds number Γ/ν. By varying the values of the viscosity ν of the fluid the vortex Reynolds numbers can be changed. The influence of the vortex Reynolds number on the residence time of the particle for a fixed value of $V_T = 0.3$ and three different values of τ_p is shown in Figure 10. R_{T_p} is the ratio of the residence time $T_p(\nu)$ for a particular value of viscosity to that of the steady case ($T_p(\nu \to 0)$), i.e.,

$$R_{T_p} = T_p(\nu)/T_p(0)\,.$$

As ν increases from zero, all these curves increase from 1 to a maximum of around $\nu = 0.0003$. As ν is increased further, the residence time decreases. Some results of this sort may be expected since as the vortex grows, the size of the trapping region decreases with time (see Figure 4); one would expect that the particle should get out of the trapping region faster. However, as the vortex grows to a larger core size, u_θ decreases with time (see Figure 1) so that the rate of spiralling outward of the particle decreases too. For small values of $\nu < 0.001$ the results suggest that the rate of decrease of the trapping region is smaller than the rate at which the particle is spiralling outward; hence the residence time increases. If ν increases further, i.e., the vortex grows faster with time, the size of the trapping region decreases faster. Therefore the particle will escape from the trapping region faster; hence the residence time should decrease. Figure 10 suggests that there is a critical value of vortex Reynolds number (about $\nu = 0.0003$) such that the residence time of the particle can be maximized in the spreading line vortex.

5. Conclusion

This paper deals with particle entrapment within ambient vortices and provides various characteristics for particle-vortex interaction, including the residence time. The motivation for this study came from recent achievements in turbulence theory showing that three-dimensional turbulent flow fields are packed with coherent elongated vortices among the small scales of many turbulent flows that live for quite a few Taylor scale-based eddy turnover times and that their scales are of the order of Taylor microscale. These vortices are modeled as a spreading line vortex.

Trajectories have been calculated for dense particles released near a steady vortex and a spreading line vortex. These show that particles released well away from the vortex will not be trapped by it, but particles released close to it will be temporarily trapped inside the trapping region of the vortex.

We have shown that the size of the trapping region is determined by the core radius of the vortex (the vortex Reynolds number) and the settling velocity V_T of the particle. Numerical simulation results show that as time increases, the vorticity is diffused outward, showing that the core size of the vortex increases and the extent of the trapping region becomes smaller. Moreover, as V_T increases, the trapping region also becomes smaller.

We have also shown that the residence time of the particle depends on three parameters, namely, τ_p, V_T, and ν. When varying one of the parameters while keeping the other two fixed, different phenomena are observed. For fixed values of τ_p and ν the residence time of the particle decreases monotonically as V_T increases. This is because when the force due to gravity increases, the particle will get out of the trapping region faster. However, for the case with fixed values of V_T and ν the results show that the residence time of the particle oscillates with τ_p.

For the case of fixed values of τ_p and V_T an optimal vortex's Reynolds number is found such that the residence time of the particle is maximized in a spreading line vortex. Of course, the length of the residence time is related to the interaction of particles with flow vorticity field, in particular, the lifetime of these intense vortical regions. As the intense vortical regions are a feature of the small-scale, dissipation range flow dynamics [*She et al.*, 1990], the length of residence time is likely to be longest when the particle parameters are comparable to the dissipation range scales, namely, the Kolmogorov scale. This is consistent with the finding of *Wang and Maxey* [1993] that the maximum increase of particle settling rate occurs when the particle parameters are made comparable to the flow Kolmogorov scales.

The results show that the small-scale flow dynamics play an important role in particle resuspension and

transport in multiphase flows. This is in contrast with the traditional approach that the large-scale, energy-containing fluid motions dominate the transport of particles, in particular, the dispersion and suspension processes. This does not invalidate the traditional approach but implies that the traditional approach may not be adequate for many aspects of multiphase flow processes.

Many questions remain to be explored. For example, the vortices are assumed to be strictly horizontal and two-dimensional in the present model, whereas in fact, the tube-like structures are very rarely strictly horizontal, and the three-dimensionality of the vortex may significantly modify the trajectory of the particles and hence affect the residence time. Also, note that the coherent structures discussed in this paper pertain to a "normal" three-dimensional turbulent flow such that their scales are of the order of Taylor microscale, i.e., too small to be resolved generally in geophysical simulations. The vortices treated in this paper are not the relatively large structures known to geophysicists as "eddies," and this paper should not be overextended to eddies-induced sediment transport and related residence time. However, the present findings are expected to be applicable to the coupling between the small scales of a turbulent flow, which can be modeled as a collection of a vortex tube and the motion of inertial particles suspended in such a flow.

Acknowledgments. Special thanks are extended to Miss W.Y. Ng and Mr. W.C. Wong who assisted with the early phases of this study. The support of the Hong Kong Research Grant Council is gratefully acknowledged.

References

Batchelor, G. K., *An Introduction to Fluid Dynamics*, 615 pp. Cambridge Univ. Press, 1967.

Browne, L. W. B., R. A. Antonia, and N. Rajagopalan, The spatial derivative of temperature in a turbulent flow and Taylor's hypothesis, *Phys. Fluids* , *26*, 1222-1227, 1983.

Chan, C. C., and J. C. H. Fung, The change in settling velocity of inertial particles in cellular flow, *Fluid Dyn. Res.*, *25*, 257-273, 1999.

Chung, J. N., and T. R. Thoutt, Simulation of particle dispersion in an axisymmetric jet, *J. Fluid Mech.*, *186*, 199-222, 1988.

Davila, J., and J. C. R. Hunt, Settling of particles near vortices and in turbulence, *J. Fluid Mech.*, in press, 2000.

Fung, J. C. H., Gravitational settling of particles and bubbles in homogeneous turbulence, *J. Geophys. Res.*, *98*, 20,287-20,297, 1993.

Fung, J. C. H., Gravitational settling of small spherical particles in unsteady cellular flow fields, *J. Aerosol Sci.*, *28*, 753-787, 1997.

Fung, J. C. H., The effect of nonlinear drag on the settling velocity of particles in homogeneous isotropic turbulence, *J. Geophys. Res.*, *103*, 27,905-27,917, 1998.

Hunt, J. C. R., T. R. Auton, L. Sene, N. H. Thomas, and R. Kowe, Bubble motions in large eddies and turbulent flows, in *Proceedings of the Conference on Transient Phenomena in Multiphase Flow*, edited by N. H. Afgan, Hemisphere, Bristol, England, U.K., 1988.

Jiménez, J., A. A. Wary, P. G. Saffman, and R. S. Rogallo, The structure of intense vorticity in isotropic turbulence, *J. Fluid Mech.*, *255*, 65-90, 1993.

Marcu, B., E. Meiburg, and R. K. Newton, Dynamics of heacy particles in a Burgurs vortex, *Phys. Fluids*, *7*, 400-410, 1995.

Maxey, M. R., The motion of small spherical particles in a cellular flow field, *Phys. Fluids*, *30*, 1915-1928, 1987.

Maxey, M. R., and S. Corrsin, The gravitational settling of aerosol particles in randomly oriented cellular flow field, *J. Atmos. Sci.*, *43*, 1112-1134, 1986.

Maxey, M. R., and J. J. Riley, Equation of motion for a small rigid sphere in a non-uniform flow, *Phys. Fluids*, *26* 883-889, 1983.

Nielsen, P., On the motion of suspended sand particles, *J. Geophys Res.*, *89*, 616-626, 1984.

Perkins, R. J., and J. C. R. Hunt, The interaction between heavy particles and an isolated vortex, paper presented at 2nd International Conference on Multiphase Flow, Kyoto, Japan, 1995.

Ruetsch, G. R., and M. R. Maxey, Small-scale feature of vorticity and passsive scalar fields in homogeneous isotropic turbulence, *Phys. Fluids*, *3*, 1587-1597, 1991.

She, Z. S., J. Jackson, and S. A. Orszag, Intermittent vortex structures in homogeneous isotropic turbulence, *Nature*, *344*, 266-268, 1990.

Ting, L., and R. Klein, *Viscous Vortical Flows: Lecture Notes in Physics*, vol. 374. Springer-Verlag, New York, 1991.

Vassilicos, J. C., and J. C. H. Fung, The self-similar topology of passive interfaces advected by two-dimensional turbulent-like flows, *Phys. Fluids*, *7*, 1970-1998, 1995.

Vassilicos, J. C., and N. Nikiforakis, Flamelet-vortex interaction and the Gibson scale, *Combust. Flame*, *109*, 293-302, 1997.

Vincent, A., and M. Meneguzzi, The spatial structure and statistical properties of homogeneous turbulence, *J. Fluid Mech.*, *225*, 1-25, 1991.

Wang, L. P., and M. R. Maxey, Settling velocity and concentration distribution of heavy particles in homogeneous isotropic turbulence, *J. Fluid Mech.*, *256*, 27-68, 1993.

Wyngaard, J. C., Atmospheric turbulence, *Annu. Rev. Fluid Mech.*, *24*, 205-233, 1992.

Yule, A. J., Investigations of eddy coherence in jet flows, in *The Role of Coherent Structures in Modeling Turbulence and Mixing*, edited J. Jinenez, pp. 188-207, Springer-Verlag, New York, 1980.

J. Fung, Department of Mathematics, Hong Kong University of Science and Technology, Clear Water Bay, Hong Kong.

(Received November 9, 1998; revised July 5, 1999;; accepted November 24, 1999.)